9. Smith, D., Neumann, G., Arvidson, R. E., Guinness, E. A. and Slavney, S., Report, NASA Planetary Data System, MGS-M-MOLA-5-MEGDR-L3-V1.0, 2003.
10. Neukum, G., Jaumann, R. and the HRSC Co-Investigator and Experiment Team, In *Mars Express: The Scientific Payload*, (ed. Wilson, A., scientific contribution: Chicarro, A.), European Space Agency Special Publication, SP-1240, Noordwijk, The Netherlands, 2004, pp. 17–35.
11. Malin, M. C. *et al.*, *J. Geophys. Res.*, 2007, **112**, E05S04; doi: 10.1029/2006-JE002808.
12. Christensen, P. R., JMARS – a planetary GIS; http://adsabs.harvard.edu/abs/2009AGUFMIM 22A.06.
13. Golombek, M. P., Tanaka, K. L. and Franklin, B. J., *J. Geophys. Res.*, 1996, **101**, 26119–26130.
14. Day, W. C., Dickerson, R. P., Potter, C. J., Sweetkind, D. S., San Juan, C. A., Drake II, R. M. and Fridrich, C. J., US Geological Survey Miscellaneous Investigations Series Map I-2627, Scale 1 : 24,000, 1998.
15. Dauteuil, O., Huchon, P., Quemeneur, F. and Souriot, T., *Tectonophysics*, 2001, **332**, 423–442.
16. Esposito, P. B. *et al.*, In *Mars* (eds Kieffer, H. H. *et al.*), The University of Arizona Press, USA, 1992, pp. 209–248.
17. Hauber, E. and Kronberg, P., *J. Geophys. Res.*, 2005, **110**, doi: 10.1029/2005-JE002407.
18. Ferrill, D. A., Wyrick, D. Y., Morris, A. P., Sims, D. W. and Franklin, N. M., *GSA Today*, 2004, **14**, 10; doi: 10.1130/1052-5173(2004)014<4:DFSAPC>2.0.CO;2.
19. Mamtani, M. A., Ghosh, A., Chaudhuri, A. K. and Sengupta, D., *Gondwana Res.*, 2003, **7**(2), 579–583.
20. Lee, J.-C., Lu, C.-Y., Chu, H.-T., Delcaillau, B., Angelier, J. and Dettontaines, B., *Terr. Atmos. Ocean. Sci.*, 1996, **7**(4), 431–446.
21. Kaymakci, N., *J. Asian Earth Sci.*, 2006, **27**, 207–222.
22. Wyrick, D., Ferrill, D. A., Morris, A. P., Colton, S. L. and Sims, D. W., *J. Geophys. Res.*, 2004, **109**, E06005; doi: 10.1029/2004JE002240.
23. Žalohar, J., T-TECTO 3.0 Professional. Integrated software for structural analysis of fault-slip data, Department of Geology, University of Ljubljana, SI-1000 Ljubljana, Slovenia, 2009.
24. Wilson, L. and Head III, J. W., *J. Geophys. Res.*, 2002, **107**(E8); doi: 10.1029/2001JE001593.
25. Quintana, S. N. and Schultz, P. H., In Proceedings of the Lunar and Planetary Science Conference, 2014, vol. 45, p. 1971.
26. Barlow, N. G., *LPI Techn. Rep.*, 1993, 93–06, Part-1.
27. Basilevsky, A. T. and Ivanov, B. A., *Geophys. Res. Lett.*, 1990, **17**(2), 175–178.
28. Twiss, R. J. and Moores, E. M., *Structural Geology*, W. H. Freeman and Company, New York, 2nd edn, 2007, p. 736.
29. Fassett, C. I., James W. and Head, J. W., *Icarus*, 2011, **211**, 1204–1214; doi: 10.1016/j.icarus.2010.11.014.
30. Yin, A., *Lithosphere*, 2012, **4**(6), 553–593.
31. Golombek, M. P. and Phillips, R. J., In *Planetary Tectonics* (eds Watters, T. R. and Schultz, R. A.), Cambridge University Press, New York, 2010, pp. 183–232.
32. Vaz, D. A., *Planet. Space Sci.*, 2011, **59**, 1210–1221.
33. Korteniemi, J., Aittola, M., Öhman, T. and Raitala, J., In Proceedings, 40th ESLAB – First International Conference on Impact Cratering in the Solar System (ed. Wilson, A.), ESA Special Publication, 2006, SP-612, pp. 193–198.

ACKNOWLEDGEMENTS. We thank the Space Applications Centre (ISRO), Ahmedabad for a project grant and the Principal, Asutosh College, Kolkata for support.

Received 1 December 2014; revised accepted 1 April 2015

KEYUR DE[1,*]
ABHIK KUNDU[1]
PRAKASH CHAUHAN[2]
NILANJAN DASGUPTA[3]

[1]*Department of Geology, Asutosh College, 92 S.P. Mukherjee Road, Kolkata 700 026, India*
[2]*Space Applications Centre (ISRO), Jodhpur Tekra, Satellite Road, Ahmedabad 380 015, India*
[3]*Department of Geology, Presidency University, 86/1 College Street, Kolkata 700 073, India*
**For correspondence.*
e-mail: de.keyur@gmail.com

Highly potassic melagranite of Bintang Batholith, Main Range Granite, Peninsular Malaysia

For decades, the Main Range Granite Province of Peninsular Malaysia has been regarded to comprise exclusively of S-type granites[1] (T. C. Liew, unpublished), which have been taken as the world standard for collisional *S*-type granite[2]. The Main Range Granite Province is believed to have formed during Triassic[3] continental collision between Sibumasu and Indochina[4] blocks subsequent to the closure of Palaeo-tethys Ocean in Early Permian. However, recently Ghani and coworkers[5,6] have found that the province also contains granites with *I*-type characteristics such as absence of Al-rich minerals such as sillimanite, cordierite, primary wedge titanite and pale green amphibole, occurrence of mafic, hornblende–clinopyroxene–orthopyroxene-bearing enclaves and increasing peraluminosity towards the most differentiated rocks.

The Malaysian Granite Province is primarily made up of two major batholiths, the Main Range batholith and the Bintang batholith (Figure 1). The Granite Province can be divided into four main facies: (i) biotite granite, (ii) amphibole-bearing granite, (iii) subvolcanic and volcanic ± dacite and orthopyroxene rhyodacite, and (4) microgranite and mesogranite associated with aplopegmatite[6]. Biotite granites are present in both batholiths, but amphibole-bearing granites are more common in Bintang batholith. *I*-type character of the Main Range Granite Province is mainly contributed by the amphibole-bearing granite. Our recent and ongoing study on the amphibole-bearing granite in Bintang batholith revealed some interesting petrographical and geochemical features present in the province, as reported in this paper.

The Bintang batholith is located in the northern part of the Main Range Granite Province, forms a N–S elongate-shaped

batholith and consists of four main plutons, namely Selama, Taiping, Bubu and Damar[3] (Figure 1). The Taiping pluton is an extremely long and narrow intrusion, regarded as an excellent example of amphibole-bearing granite in the Main Range Granite Province[3,5]. The granites of Taiping pluton can be further divided into two smaller sub-facies, the amphibole-bearing Buloh Pelang granite and Kupang granite[7] (melagranite), and the minor megacrystic tourmaline-bearing Maxwell Hill microgranite[3].

The amphibole-bearing melagranite of Taiping pluton is coarse-grained and porphyritic. Large white to grey euhedral K-feldspar phenocrysts are widespread and megacrysts (about 5 cm) can be found, but their distribution is highly erratic. The rocks also contain various mafic microgranular enclaves and mafic xenoliths containing feldspar, hornblende, clinopyroxene and orthopyroxene. Most of them are dark coloured and contain high amount of mafic minerals. The presence of enclaves suggests mingling with small proportion of mafic magma, whereas the presence of xenoliths could be related to assimilation of sedimentary or pyroclastic rocks by the granitic magma during intrusion[8]. Euhedral K-feldspar phenocrysts are often found aligned parallel to the microgranular enclaves.

The common mineral assemblage in the amphibole-bearing melagranite is K-feldspar + plagioclase + biotite + quartz + amphibole ± orthopyroxene ± clinopyroxene. Accessory minerals are apatite, zircon, opaque minerals, titanite and allanite. The twinned, perthitic K-feldspar phenocrysts show a patchy texture. Inclusions of plagioclase, biotite and quartz indicate K-feldspar growth during magma evolution. Plagioclase phenocrysts with patchy zoning are also sometimes found. Quartz is small and anhedral, and tiny acicular rutile has been observed in quartz. Pyroxene relics are often found in amphibole. Titanite is often shapeless and strained though euhedral grains do occur.

Mineralogy of the amphibole-bearing melagranite clearly is different from the Main Range Granite proper. The melanocratic character of the amphibole-bearing melagranite suggests a higher proportion of biotite (up to 25%), which is different from the Main Range Granite proper (around 10%). Also compared to the amphibole-bearing melagranite, the typical Main Range Granite lacks amphibole, orthopyroxene, clinopyroxene and possibly titanite.

We have collected and analysed 50 new samples from Taiping pluton. Geochemical analyses were carried out at Acme Analytical Laboratories, Canada and representative analyses are given in Table 1. The amphibole-bearing melagranites are metaluminous to weakly peraluminous (A/CNK = 0.65–1.06) with an intermediate SiO_2 range from 59.2 to 65.5 wt%. They have a high magnesium number (54.24–66.38) and hence their CaO/MgO ratio falls between 0.41 and 1.09. The rocks can be considered as ultrapotassic, following ultrapotassic chemical screening[9] ($K_2O > 3$ wt%, $K_2O/Na_2O > 2$ wt% and MgO > 3 wt%).

The amphibole-bearing melagranites are high in most of the incompatible elements

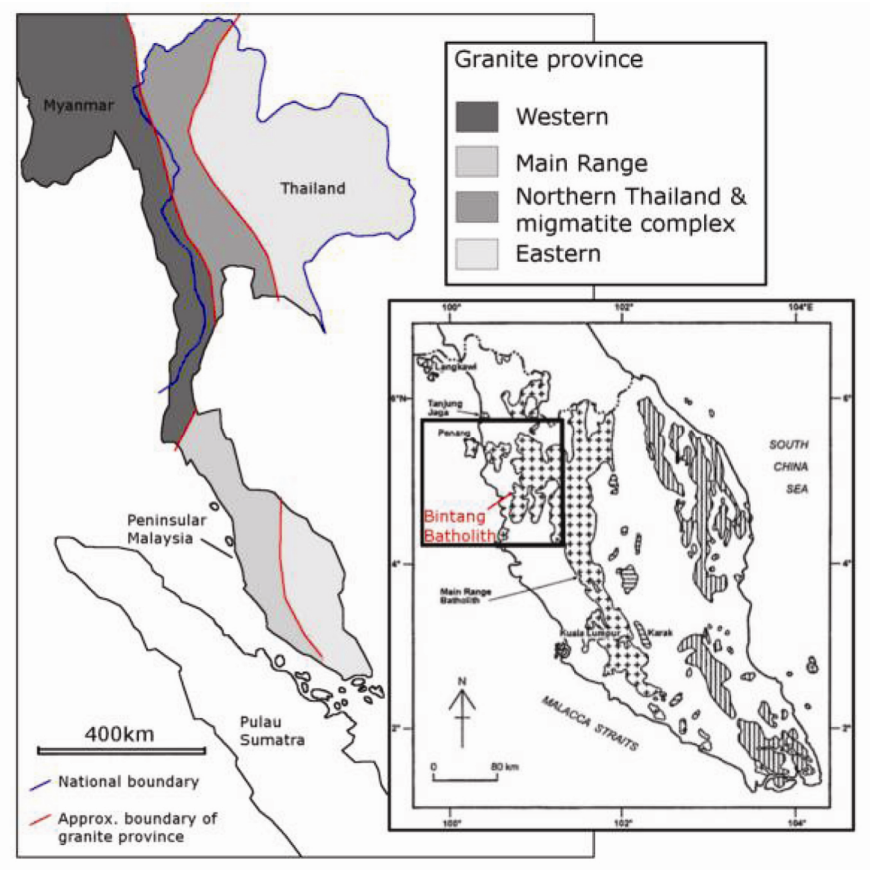

Figure 1. Map showing granite provinces from Thailand, Myanmar and Peninsular Malaysia. (Lower right) Location of Bintang batholith in Peninsular Malaysia. Maps modified from Cobbing *et al.*[3].

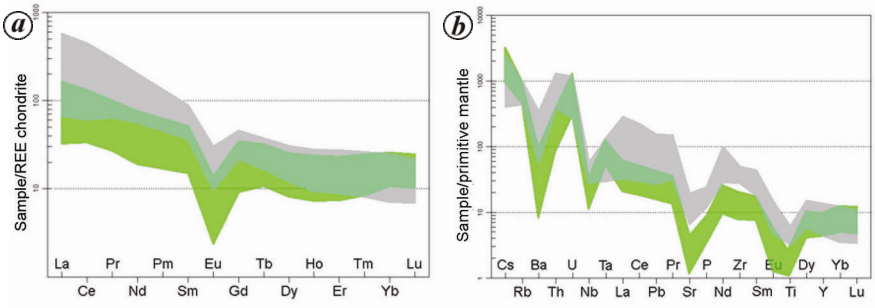

Figure 2. Geochemical comparison between Taiping pluton amphibole-bearing melagranite and typical Main Range granite (Kyaw Kyaw Nyein, unpublished). ***a***, Chondrite normalized REE plot. ***b***, Primitive mantle-normalized multi element diagram. Grey, Taiping pluton amphibole-bearing melagranite; Green, Main Range Granite. Trace and rare earth elements are in ppm.

Table 1. Selected major and trace element data

Area	Batu Kurau	Bukit Berapit		Lenggong Valley	
Label	BK-D	BB-1	BB-2	BH3 2B	BH1 6A
SiO_2	61.4	63.5	64.8	63.1	60.2
Al_2O_3	11.36	13.53	12.86	15.3	16.13
FeO	6.15	4.91	4.75	3.84	4.51
Fe_2O_3	0.76	0.61	0.59	0.47	0.56
CaO	5.55	1.75	1.45	3.16	3.41
MgO	6.39	3.66	3.51	3.02	3.63
Na_2O	1.20	1.61	1.35	2.01	2.37
K_2O	4.89	7.00	7.31	6.3	5.31
MnO	0.16	0.08	0.07	0.05	0.06
TiO_2	0.97	1.12	1.06	0.85	1.04
P_2O_5	0.36	0.38	0.35	0.33	0.39
LOI	1.12	0.71	0.78	0.91	1.58
Sum	100.30	98.85	98.88	99.35	99.18
Ba	987	368	379	1904	1620
Cs	12.5	49.9	51.7	12.5	11.6
Ga	16.1	20.8	18	18.4	20.8
Hf	11.4	15.3	13.5	10.4	11.6
Nb	27.6	44.7	45.2	22.7	26.1
Rb	321	610.3	617.8	334.5	312.5
Sr	165.1	100.3	93	328.6	383
Ta	2.1	6	5	1.4	1.3
Zr	392.2	500.2	514.8	362.4	433.2
Y	44.1	60.9	57.4	23.3	25.4
Th	107.6	92.3	85	22.3	39.4
U	18.1	35.9	34.7	5.4	6.5
Pb	11.3	31.3	13.2	11.4	7.4
La	61.8	17.5	17	28.8	58
Ce	129.8	50.7	49.4	63.9	123.2
Pr	15.45	8.17	7.45	8.18	14.89
Nd	60.6	38.1	35.5	35.3	61.2
Sm	13.51	12.25	12.34	7.43	11.05
Eu	1.22	0.59	0.67	2.01	2.17
Gd	10.36	11.58	10.64	6.09	8
Tb	1.52	1.81	1.76	0.9	1.12
Dy	7.22	10.26	9.53	4.47	5.82
Ho	1.64	2.28	2.19	0.94	1
Er	4.15	5.97	5.95	2.19	2.74
Tm	0.6	0.92	0.88	0.32	0.33
Yb	4.16	5.4	5.82	1.7	2.14
Lu	0.55	0.86	0.84	0.27	0.3
Co	18.4	14	11	11.4	13.7
Cu	11.2	4.3	6.4	12.4	10.6
V	104	113	107	81	103
Zn	42	66	56	57	54
Ni	52.9	26.8	27.5	28.6	27.7
Cr	526.8	266.8	376.3	369.5	301.0

(Rb, Ba, Th, La, Ce, Zr) and transition metals (Cr, Ni, V, Zn), generally enriched in Th relative to U with Th/U ratio spread between 2.38 and 12.8 and high Rb/Sr ratio (0.82–6.64). The chondrite normalized rare earth element (REE) diagram[10] (Figure 2) shows high ∑REE, high LREE/HREE ratios, elevated LREE content and moderate Eu-anomaly (Eu/Eu*). The primitive mantle normalized multi-element variation diagram[11] (Figure 2) shows elevation in some LILE such as Cs, Rb, Ba and HFSE such as Th, U, Zr, but shows clear Ta–Nb–Ti (TNT) negative anomaly relative to the adjacent elements. Significant features are: (i) moderately enriched LREE patterns, (ii) flat HREE patterns, (iii) weak Eu depletion, (iv) negative Ba, Nb, Ta, Sr and Ti anomalies and (v) positive Cs, Rb, Th, U, Nd, Zr, Sm anomalies. The calculated apatite saturation temperature[12] for the melagranite ranges from 928.8°C to 1014.8°C. This temperature is significantly higher than that of granitoid melt generated by melting of sedimentary source (experimentally, ≤ 700°C)[13].

Although petrography and geochemistry data suggest weak sedimentary signature, the melagranites show high initial $^{87}Sr/^{86}Sr$ isotope ratio (ISR), from 0.715 to 0.726 (refs 3 and 13; assuming the age of the granite is 220 Ma (ref. 14), a common accepted age for Main Range Granite Province). ISR values are thought to reflect the variations in composition and source material age of the magma[15]. High initial ISR on the rocks could reflect partial melting of portions of older lower crustal lithosphere to generate magma[15]. Partial fusion of supracrustal metasedimentary rocks could produce high ISR magma, but it cannot produce magma composition like those of the melagranite[15]. A more possible explanation is partial fusion of mafic volcanic rocks[15], which explains the melagranite magma petrography and geochemical composition and the presence of mafic microgranular enclaves.

Tectonic discrimination diagram[16] (Figure 3) shows that most of the melagranites fall within Group 1 (contribution from subduction). As the tectonic model for Peninsular Malaysia currently does not support subduction at the time of melagranite emplacement, it is possible for the subduction contribution to be inherited from an underplated source formed from previous tectonic event, which may or may not pre-date the melagranite age significantly. Such assumption is supported by the ISR data, explaining how the melagranite with 'subduction geochemical signature' can be produced in a different setting (transitional to a collision setting), or at a different time.

To fit the melagranite to the current tectonic scenario, we suggest a minor extension episode to occur during the early Sibumasu–Indochina collision on the Sibumasu side (Figure 4). Slab pull created by subduction of a higher density oceanic lithosphere could result in extensional deformation within the subducted slab below the area of the slab bend[17]. Underplated source will then be heated by the upwelling of asthenospheric mantle from lithosphere necking, generating

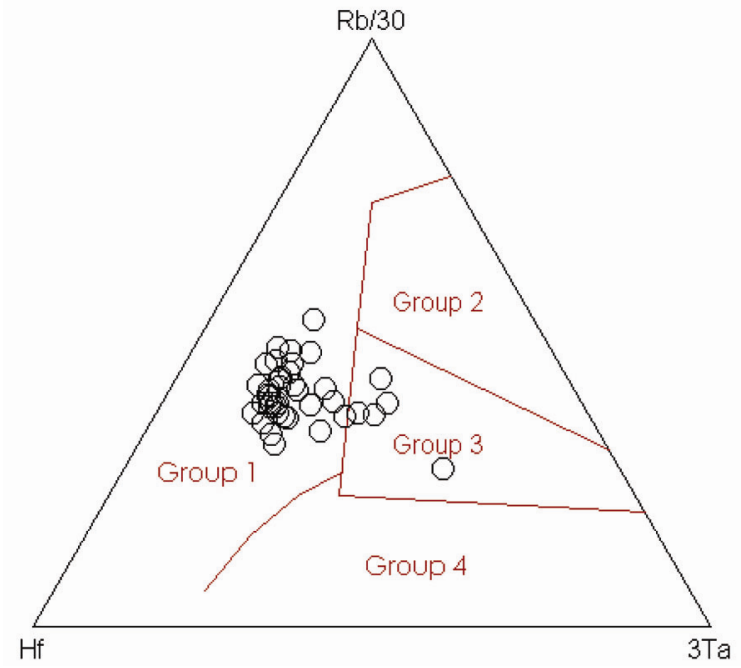

Figure 3. Tectonic discrimination diagram according to Harris *et al.*[16] (trace elements in ppm). Group 1: Pre-collision calc alkaline intrusions mostly derived from mantle modified by a subduction component. Group 2: Syn-collision peraluminous intrusions which may be derived from the hydrated bases of continental thrust sheets. Group 3: Late or post-collision calc-alkaline intrusions which may be derived from a mantle source but undergo extensive crustal contaminations. Group 4: Post-collision alkaline intrusions which may be derived from mantle lithosphere beneath the collision zones.

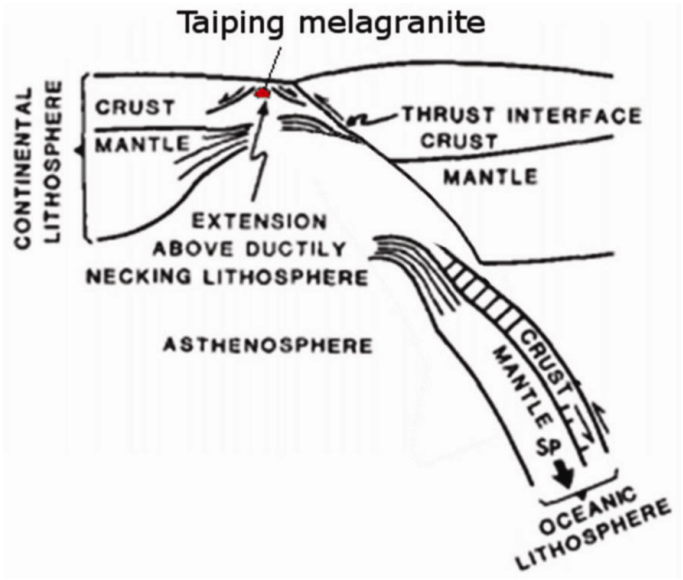

Figure 4. Model sketch according to Sacks and Secor[17], reminiscent of a slab break-off process.

the melagranite magma. Such extension episode will be short-lived if both plates continue to converge, as the compressive tectonic regime will be re-established[17], causing this particular event to be obscured.

Thus we have reported here a highly potassic amphibole-bearing melagranite partially surrounded by *S*-type Main Range tin-bearing granite of Late Triassic age. The amphibole-bearing melagranite contains hornblende, clinopyroxene and orthopyroxene, and its geochemistry indicates intermediate to high SiO_2 content, high Rb/Sr, Th, LREE, LILE and low Ca, Na. The analyses presented here suggest that the Main Range Granite Province is composed of a wider range of granitic and associated rocks (from 59.2% to 77% SiO_2) contrary to previous views that it is composed of restricted felsic magmatism (65% to 77% SiO_2).

With these findings, the tectonic scenario of Peninsular Malaysia needs to be carefully revised, especially the collision event of the Triassic period between Sibumasu and Indochina blocks, to accommodate the occurrence of these highly potassic amphibole-bearing melagranites. The primitive character of the amphibole-bearing melagranite compared to the typical Main Range Granite suggests that the former has mantle contribution, in contrast to the accepted crustal origin of the typical Main Range Granite. High Mg number (54.2–66.4), Cr (233–568 ppm) content and high Th/U (2.38–12.8), Rb/Sr (0.82–6.64) ratios support mantle contribution to the amphibole-bearing melagranite magma.

1. Hutchison, C. S., *Geol. Rundsch.*, 1994, **83**, 388–405.
2. Pearce, J. A., Harris, N. B. and Tindle, A. G., *J. Petrol.*, 1984, **25**, 956–983.
3. Cobbing, E. J., Pitfield, P. E. J., Darbyshire, D. P. F. and Mallick, D. I. J., *The Granites of the South–East Asian Tin Belt*, British Geological Survey, Keyworth, 1992.
4. Mitchell, A. H. G., *Geol. Soc. Malays. Bull.*, 1977, **9**, 123–140.
5. Ghani, A. A., *Geosci. J.*, 2000, **4**, 283–293.
6. Ghani, A. A., Searle, M., Robb, L. and Chung, S.-L., *J. Asian Earth Sci.*, 2013, **76**, 225–240.
7. Burton, C. K., *The Geology and Mineral Resources of The Baling Area, Kedah and Perak*, Geological Survey West Malaysia, Ipoh, 1970.
8. Jones, C. R., *The Geology and Mineral Resources of The Grik Area, Upper Perak*, Geological Survey West Malaysia, Ipoh, 1970.
9. Foley, S. F., Venturelli, G., Green, D. H. and Toscani, L., *Earth-Sci. Rev.*, 1987, **24**, 81–134.
10. Boynton, W. V., In *Rare Earth Element Geochemistry* (ed. Henderson, P.), Elsevier, Amsterdam, 1984, pp. 63–114.
11. Mcdonough, W. F. and Sun, S. S., *Chem. Geol.*, 1995, **120**, 223–253.
12. Harrison, T. M. and Watson, E. B., *Geochim. Cosmochim. Acta*, 1984, **48**, 1467–1477.

13. Liew, T. C. and McCulloch, M. T., *Geochim. Cosmochim. Acta*, 1985, **49**, 587–600.
14. Oliver, G., Zaw, K., Hotson, M., Meffre, S. and Manka, T., *Gondwana Res.*, 2014, **26**, 132–143.
15. Arth, J. G., Zen, E. A., Sellers, G. and Hammarstrom, J., *J. Geol.*, 1986, **94**, 419–430.
16. Harris, N. B., Pearce, J. A. and Tindle, A. G., *Geological Society*, London, Special Publications, 1986, **19**, 67–81.
17. Sacks, P. E. and Secor, D. T., *Geology*, 1990, **18**, 999–1002.

ACKNOWLEDGMENT. The work is partly sponsored by University Malaya UMRG Grant no. RG263/13AFR and UM/MOHE High Impact Research Grant (UMC/HIR/MOHE/SC/27). The samples for this study are taken from core sample of Archeological research of Bukit Bunuh, Peninsular Malaysia: Grant no. 1002/Parkeo/910202DE2012 headed by Prof. Mokhtar Saidin from Univesity Sains Malaysia. Dr Zuhar Zahir is thanked for providing the granite samples. Field work for this project is partly sponsored by PPP grant from University Malaya (PV087-2012A). Armstrong Hilton Limited is acknowledged for editing the English.

Received 3 December 2014; revised accepted 21 April 2015

LONG XIANG QUEK[1]
AZMIAH JAMIL[1]
AZMAN A. GHANI[1,*]
MOKHTAR SAIDIN[2]

[1]*Department of Geology, University of Malaya, Kuala Lumpur, 50603 Malaysia*
[2]*Centre for Global Archaeological Research Universiti Sains Malaysia, Penang, 11800 Malaysia*
**For correspondence.*
e-mail: azmangeo@um.edu.my

Species diversity–primary productivity relationships in a nitrogen amendment experiment in grasslands at Varanasi, India

The accelerated loss of biodiversity due to the land use and global climate changes has proved detrimental to ecosystem functioning (i.e. litter decomposition, nutrient cycling, energy storage and flux, ecosystem services, etc.). It has attracted intensive experiments during the past four decades, because primary productivity (P) as a measure of ecosystem functioning may or may not be closely coupled with species diversity (D)[1–7]. Nevertheless, relationships between the above have been attributed to changes in the size and composition of competitive plant functional groups under varied resource availability and diverse ecological incidents[7].

Several experimental and theoretical studies have led to vital debates on *D–P* relationships[6–9]. The reviews by Waide *et al.*[10] and Mittelbach *et al.*[11] showed variations in the shape of *D–P* relationships, depending on the study systems, spatial scales, environmental factors and competitive ability of species, and functional group compositions[7]. Positive *D–P* relationship was reported in many studies[3,12–14]. Nutrient input studies have suggested higher productivity with lower species diversity[9,15,16]. On the other hand, some biodiversity experiments showed a reduction in species diversity due to decline in productivity[4–8]. Several other trends have been suggested, including none[6] or idiosyncratic relationships between species diversity and primary productivity[17]. Many studies, using correlations across different sites or nutrient additions, suggested a hump-shaped curve for the relationship between diversity and productivity (see refs 10, 11 for details). Grime[1] was the first to note a hump-shaped relationship between diversity and productivity. Majority of the studies, including meta analysis suggested that unimodal *D–P* relationship is more prevalent in natural communities[18], while others suggested that a monotonic positive and linear relationship is more common[4,19,20]. Hence, the relationship between plant diversity and primary productivity has continued to be an essential issue in ecological and environmental sciences[3–9].

In view of the aforesaid debate, the present study was conducted to answer the following questions: (i) Does species diversity exhibit a linear relationship with primary productivity? (ii) Does plant functional group composition determine the *D–P* relationships in nitrogen (N)-amended experimental plots located in a dry tropical environment of India?

The study was based on three doses of N-amendment (control, 6 and 12 g N m^{-2} $year^{-1}$) experienced by the herbaceous grassland vegetation from January 2007 to December 2010. The doses 6 g and 12 g N are referred to as low and high N treatments respectively. In this study we used 6 and 12 g N m^{-2} $year^{-1}$ because in our previous study the application of 6 g N m^{-2} $year^{-1}$ did not saturate the soil. In this experiment, a total of 135, 1 × 1 m plots (15 locations × 3 treatments × 3 replicates), all situated on plain, alluvial grounds within the campus of the Banaras Hindu University (BHU), Varanasi, India (24°180′N and 83°03′E and 76 m amsl) were used. The soil is moderately fertile being low in soil-C (0.84 ± 0.07%) and soil-N (0.08 ± 0.01%). The soil pH is neutral to alkaline (7.19 ± 0.12). Data were collected in the year 2011. Species diversity was calculated using Shannon–Wiener equation[21]. The number of species/m^2 was used for computing the species richness[22]. Sheldon[23] equation was used to quantify the evenness. Aboveground peak herbaceous biomass was considered as a measure of primary productivity[6,24,25]. These parameters were determined for each N level in each season. Contribution of diverse species to total plant biomass was assessed by species separation in June, September, December and March which corresponded respectively, with the start of vigorous growth of herbaceous vegetation at the beginning of the rainy season, the time when rainy-season vegetation is at its best, the mid-winter phase of relative inactivity, and the period when flowering and fruiting of the plants during the summer season show renewed but limited growth[24]. The average values of the three growing seasons were used to establish the *D–P* relationships using SPSS statistical software.

The number of species, relative biomass and functional groups represented